Innovative Steel Pennon Plate-Headed Stud of Shear Connectors for Composite Structures

Rahul Tarachand Pardeshi[*], Prakash Abhiram Singh, Yogesh Deoram Patil

Department of Civil Engineering, Sardar Vallabhbhai National Institute of Technology, Surat, Gujarat, India

Abstract

This study proposes an innovative pennon plate-headed stud of shear connectors. The proposed stud consists of two triangular-shaped steel plates on both sides of the headed stud; it is expected to increase the shear capacity of a steel-concrete composite connection. Nonlinear finite element analysis is carried out using ABAQUS to analyze the response of 54 models of PPH studs. A full factorial design and the analysis of variance are employed in the design of experiments (DOE). The impacts of factors and their interactions, such as the thickness and height of the pennon plates, concrete grades, and stud diameters, are captured by using $3^3 \times 2^1$ DOE with a 5% significance level. The results show that the ultimate shear resistance is increased apparently. Additionally, the concrete grade and stud diameter significantly influence the capacity of the connection. Moreover, connection slip is greatly affected by concrete grade, the height of the plate, and the interaction between plate thickness and height.

1. Introduction

Fig. 1 shows a composite construction that consists of steel beams and reinforced concrete (RC) slabs. In this composite construction, longitudinal shear forces are transmitted across the interface through the mechanical action of shear connectors. Composite structures are advantageous for reducing the overall structural weight, boosting load capacity, and reducing construction depth. Therefore, it is widely adopted in the construction of modern buildings and highway bridges. Headed stud shear connectors are typically utilized for transferring longitudinal shear in composite beams [1]. The shear resistance of the connection in composite elements is primarily influenced by the stud shear resistance and the compressive strength of the concrete slab [2]. The slip capacity of the connection at the steel-concrete beam interface affects the overall structural behavior [3].

Pushout tests have long been the primary method for determining the load-slip behavior of shear connectors in composite structures. Although experimental displacement with load increment provides helpful information through the pushout test, the required experimental procedure is either impractical or prohibitively expensive for studying a large number of parameters.

Sun et al. [4] experimentally investigated the performance of a headed stud welded to a composite deck for the effect of decking type, presence, and direction of rib on shear capacity. Deng et al. [5] combined headed studs and perfobond ribs to enhance composite structure shear behavior. Konrad and Kuhlmann [6] investigated the bearing resistance of headed studs used in trapezoidal steel sheeting to determine the effect of the stud's location in the trough and other geometric factors on the failure mode. Chen et al. [7] investigated the thermo-structural response of shear connectors implanted in composite slabs with sheeting parallel to a steel beam. Eurocode 4 [8] produced a conservative estimate of the ultimate strength of the material at

---

* Corresponding author. E-mail address: rahultpardeshi@gmail.com

elevated temperatures. Imagawa et al. [9] studied the effect of heat on the performance of headed stud shear connectors. The study revealed that marginal heating affects the maximum shear resistance of headed studs, but it significantly reduces the slip constant during and after the fire.

Shim and Kim [10] carried out an experimental study to reduce the number of studs at the end joint to reduce congestion and enhance the constructability of the joint. The study recommended the new bent stud to improve the bond strength of studs effectively in joint regions. Suwaed and Karavasillis [11-12] developed a novel bolted demountable shear connector for precast structures. It aids in speedy construction and disassembly. The shear strength increases by 10% compared to conventional headed shear connectors. Also, the stiffness, slip capacity, and resilience of the slab become better.

Pathirana et al. [13] experimentally investigated the load-slip behavior of welded shear studs and blind-bolt connectors in normal concrete and grout. The study revealed the efficiency of the welded shear studs with grouting latter for retrofitting works. Parametric studies showed an enhanced shear capacity with increased grout strength and height of the studs. Yang et al. [14] advanced the bolted shear studs by assembling a short bolt, a long bolt, and a coupler. However, the static pushout tests displayed shank failure of short bolts under the couplers.
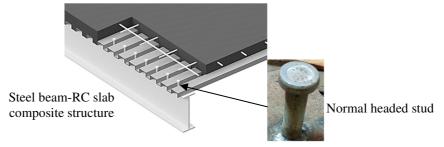

Fig. 1 Typical arrangement of a steel-concrete composite connection [1]

In comparison, analytical approaches can forecast the nonlinear response of the number of pushout tests with shear connectors of complex geometry. Mirza and Uy [15] used finite element (FE) analysis to investigate the effects of various strain regimes on the strength prediction and load-slip behavior of shear connections in composite structures. Qureshi et al. [16] investigated the shear effect of single and double studs in trough-profiled steel sheeting using FE analysis. Vigneri et al. [17] showed the significance of the location of plastic hinges in headed stud shear connections and slip considerations that relate to the progressive crushing of concrete in steel beam-profile sheeting concrete slab ribs through numerical simulations.

By using an FE technique, Mia and Bhowmick [18] created a system using a pushout specimen-based fatigue life estimation system for headed shear stud connections. The primary critical aspect in composite steel beam-RC slab construction is a shear failure at connection. Pardeshi et al. [19] proposed an innovative shear connector called a concave type shear connector made up of regular reinforcement to save stud steel material and easy to speedy in-situ fabrication of shear connector.

Due to the cylindrical shape and small circular section of the regular-headed stud, it has limited shear resistance and moment of inertia. Generally headed studs are failed in shear due to a high concentration of stresses near the bottom of the stud [19]. The composite action of the composite structure is completely dependent upon the shear capacity of the shear connector. The composite action is directly co-related to the shear capacity of the shear connector. The stronger the shear resistance gets, the better the capacity of the composite structure will be. The capacity of the conventional headed stud shear connector is low, hence, many studs are required in the composite beam to provide the desired shear resistance.

The current study aims to propose an innovative pennon plate-headed (PPH) studs shear connector for better shear resistance of composite connection than regular circular-headed stud shear connectors. The triangular-shaped steel plates similar to the pennon have been welded to the shank of a standard-headed stud shear connector to form the PPH stud. Then, the base of PPH studs should be welded to the flange of the steel beam and embedded in a concrete slab when in use.

This study uses FE analysis to explore the performance of PPH studs in composite action for strength and load-slip behavior over the standard-headed stud shear connector. The parametric studies using full factorial design of experiments (DOE) have been investigated for analyzing the effect of parameters on shear connection performance. The effect of the pennon plate thickness (t), the height of the pennon plate (h), different grades of concrete (f_c), and stud diameter (d) as key parameters, and their interactions are considered in the investigation. The present study is the first extensive research on the steel plates welded to the shank of the stud in composite structures for their strength and load-slip performance. Fig. 2 depicts the construction of the proposed PPH stud with a total height (H) of 100 mm.
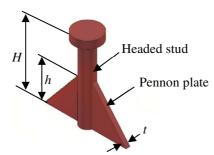

Fig. 2 The proposed PPH studs
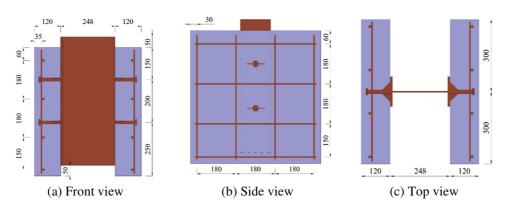
2. Shear Connector Finite Element Model

(a) Front view (b) Side view (c) Top view

Fig. 3 The geometry of specimens (all dimensions are in mm)

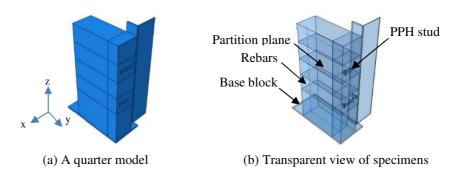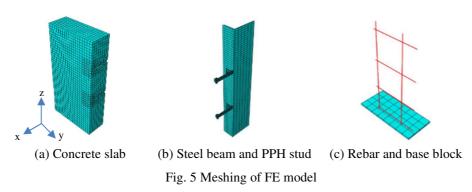(a) A quarter model (b) Transparent view of specimens

Fig. 4 3D model of specimens

The pushout test is modeled using FE analysis [20]. The shear connectors, steel beams, reinforcement, and concrete slabs are the influential components of the shear connection behavior in the composite beam. Precise interaction between components is essential to get accurate results as geometric and material nonlinearity is involved in FE analysis. The specimen geometries are shown in Fig. 3. Figs. 4 (a)-(b) show a quarter model and a transparent view of specimens. FE simulation is made possible by modeling a quarter of the specimen because of the symmetry in the specimens. FE analysis results of PPH studs are compared with regular circular-headed stud analysis results to check the comparative performance. Also, the load-slip capacity of PPH studs and the conventional 19 mm regular circular-headed stud for C40 and C50 grade concrete are compared by using finite element analysis.

2.1. Element type and meshing

The concrete slab and a steel beam section are meshed using the C3D8R solid element. The rebar is used as the T3D2 truss element in modeling. The base block is described as a rigid element R3D4. The complex geometry caused by PPH studs near the interface between concrete and stud, and the stud with plate requires tetrahedron elements (C3D10) to resolve the complexity of the analysis. The FE modeling of the specimens is shown in Fig. 5. Initially, the assumed mesh size around the shear connector hole area is 5 mm and 40 mm in the rest of the concrete area. The finite element simulation showed a variation of 12% in the results. Hence, the mesh size of 4.5 mm was considered for the concrete slab area around the stud hole and 25 mm in the rest of the concrete slab for the accuracy of mesh convergence.

(a) Concrete slab   (b) Steel beam and PPH stud   (c) Rebar and base block

Fig. 5 Meshing of FE model

2.2. Constrain conditions and interaction

The components are arranged and appropriately positioned to create the specified model. The interactions between components are described using appropriate constraints. The tie constraint is applied to tie nodes of the stud surface to the concrete slab hole surface around the stud, as shown in Fig. 6(a). The surface between the concrete and steel beam flange is connected using a surface-to-surface contact interaction as shown in Fig. 6(b); the contact interaction utilized no friction as these parts are assumed to be lubricated. The tie constraint is applied to the steel beam-stud base interface in Fig. 6(c), considering perfect welding between two surfaces. The rebars are placed in the concrete slab subjected to the embedded constraint. At the contact surface between the base block and the concrete slab, contact interaction (0.15) is used as per the Nguyen and Kim [21] analytical study to justify the boundary conditions.
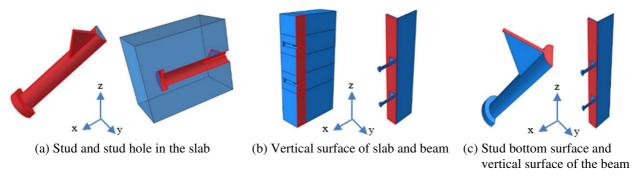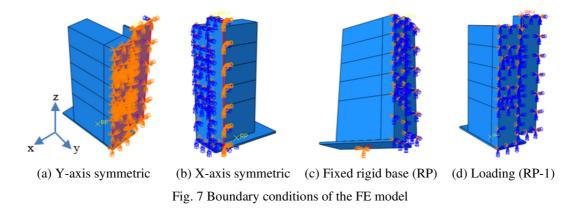

(a) Stud and stud hole in the slab   (b) Vertical surface of slab and beam   (c) Stud bottom surface and
                                                                                      vertical surface of the beam

Fig. 6 Constrain and interaction surfaces

2.3. Boundary conditions and loading

Since the geometry of the pushout test setup is symmetric, the symmetric boundary condition (SBC) is applied to the specimen surfaces of symmetric planes in Figs. 7(a)-(b). Because the rigidity of the base block is not movable, all degrees of freedom of the rigid base reference node are constrained in Fig. 7(c). Loading is applied as a downward displacement to the top surface of the steel beam, as shown in Fig. 7(d). The amplitude function is used to increase the applied displacement linearly. The dynamic explicit method is used in this investigation since it effectively deals with discontinuous and contact problems.

For validation of the FE model, the load is applied with a displacement of 16 mm with a time one amplitude function, whereas in the parametric studies, the load is applied with a displacement of 25 mm with a time 1.56 amplitude function, keeping the same rate of loading.

(a) Y-axis symmetric   (b) X-axis symmetric   (c) Fixed rigid base (RP)   (d) Loading (RP-1)

Fig. 7 Boundary conditions of the FE model

2.4. Concrete material model and properties

Uniaxial stress-strain curves for compressive and tensile concrete behavior are shown in Fig. 8(a) and (b), respectively. The concrete damage plasticity (CDP) model from ABAQUS simulated the nonlinear concrete behavior [20]. Concrete compression has three parts of the curve. The first portion is in the elastic range of the relative limit state. The relative limit stress for the first linear portion of the curve is set to 0.4 f_{cm} and $f_{cm} = 0.8 f_{cu}$, where f_{cm} and f_{cu} are cylindrical and cube compressive strength of concrete in MPa, respectively. As per Eurocode 2 [22], the value of strain (%) corresponding to f_{cm} is $\varepsilon_{c1} = 0.7 f_{cm}^{0.31}$. The initial Young's modulus E_{cm} [22] is determined by:

$$E_{cm}(MPa) = 22 \times 10^3 \times (0.1 f_{cm})^{0.3} \tag{1}$$

In concrete, the Poisson's ratio is 0.2.

In the second segment, the nonlinear parabolic component of the curve begins at the relative limit of stress 0.4 f_{cm} and progresses to the concrete capacity f_{cm}. The nonlinear parabolic segment of the curve [22] follows:

$$f_{ci} = \left(\frac{\kappa \xi - \xi^2}{1 + (\kappa - 2)\xi} \right) f_{cm}, \; for \; 0.4 f_{cm} < f_{ci} < f_{cm} \tag{2}$$

where $k = 1.1 E_{cm} \times (\varepsilon_c / f_{cm})$, $\xi = \varepsilon_{ci} / \varepsilon_c$, and $0.4 f_{cm} / E_{cm} < \varepsilon_{ci} < \varepsilon_c$.

The third section of the curve is the section from f_{cm} to a value of αf_{cm}. As per Eurocode 2 [22] and Ellobody et al. [23], factor α varies between 0.5 to 1 depending on the compressive strength of the concrete. For the present study, α = 0.85 is referred from Nguyen and Kim [21] for good calibration of FE results. The third section ends at $\varepsilon_{cu} = 0.0035$ as per guidelines provided by Eurocode 2 [22], but for good agreement of experimental results with FE analysis, $\varepsilon_{cu} = 0.01$ is adopted in the detailed parametric investigation as per Nguyen and Kim [21].

The tension curve for concrete can be divided into two segments. As per specifications given by Eurocode 2 [22], the tensile curve exhibits linear behavior up to the highest stress, it is referred to as the tensile strength of concrete f_{ctm} by:

$$f_{cm} = 0.3 (f_{cm} - 8)^{2/3} \tag{3}$$

The second segment is called tension stiffening.

$$f_{ct} = f_{ctm} (\varepsilon_{ctr} / \varepsilon_{ct})^{0.4}, \; \varepsilon_{ctr} < \varepsilon_{ct} < \varepsilon_{ctu} \tag{4}$$

The tension stiffening is defined by the weakening function as per Eq. (4) given by Wang and Hsu [24] up to the total tensile strain, $\varepsilon_{ctu} = 0.005$ [21]. ε_{ctu} is taken into account after cracking strain ε_{ctr} at f_{ctm} as shown in Fig. 8(b).

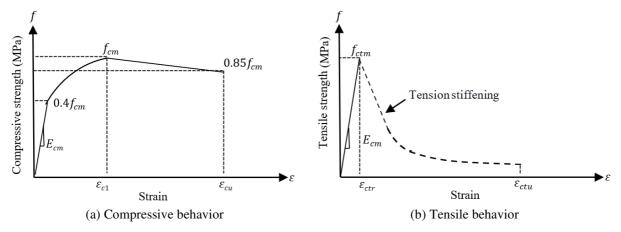(a) Compressive behavior   (b) Tensile behavior

Fig. 8 Stress-strain relationship for concrete material

Concrete material nonlinearities in compression and tension are simulated by using damaged plastic models based on uniaxial material constitutions. The damage variable $D_C = 1 - (f_{ci} / f_{cm})$ for compression damage and $D_t = 1 - (f_{ct} / f_{ctm})$ for tension damage is specified as a phase of modulus deterioration. Flow potential eccentricity (0.1), material dilation angle (30), strength ratio in biaxial to uniaxial condition (1.16), and deviatoric cross-section parameter ($k = 0.667$) are used to define the CDP (concrete damage plasticity) model. The yield surface in the deviatory plan is derived from the Mohr-Coulomb yield surface function in cylindrical coordinates for various values of k ranging from 0.5 (Rankine yield surface) to 1 (von Mises yield surface) [25]. ABAQUS user manual suggested values for flow potential eccentricity = 0.1 and biaxial/uniaxial compressive strength ratio as 1.16 [20]. A dilation angle of 30° is iteratively adjusted to match the findings of push-out tests. Several values of Kc range from 0.5 to 1. Table 1 describes the properties of concrete used in verification and parametric study.

Table 1 Concrete properties

Concrete properties	Verification model [25]	Grade of concrete		
		C30	C40	C50
f_{cm} (MPa)	26.2	38	48	58
ε_{c1} (%)	-	2.2	2.3	2.45
f_{ctm} (MPa)	2.45	2.9	3.5	4.1
E_{cm} (GPa)	21.5	33	35	37

2.5. Reinforcement, structural steel, and PPH stud properties

The bi-linear curve is used to depict the stress-strain relationship of structural and reinforcing steel as shown in Fig. 9(a). The material properties used for the PPH shear connector (a stud and two pennon plates made of the same material) and structural and reinforcing steel are described in Table 2. The material modeling for PPH stud is done by the tri-linear stress vs. strain curve, as presented in Fig. 9(b). This research aims to study the behavior of the connector; hence, reinforcement in pushout specimens does not carry the load and only acts as confinement to concrete.

More accurate material behavior is obtained using a Trilinear stress-strain curve than a bi-linear curve. As headed stud has prime importance in shear action for the pushout test; therefore, for higher accuracy tri-linear curve approach is utilized in modeling PPH stud material properties. The behavior of the material is elastic initially. After reaching the elastic limit, the yielding of the material occurs as a result of strain-softening. The stress at yield (σ_{ys}) is calculated at $\varepsilon_{ys} = 0.2\%$, and the ultimate stress (σ_u) is determined at $\varepsilon_u = 0.6\%$ [21]. The material damage and failure options in the material model for shear stud connections are used as input to model the post-ultimate stress behavior of the. The damage initiation criterion and the damage evolution response are included in modeling material failure, as shown in Fig. 10.

(a) Reinforcement and structural steel   (b) Shear connector
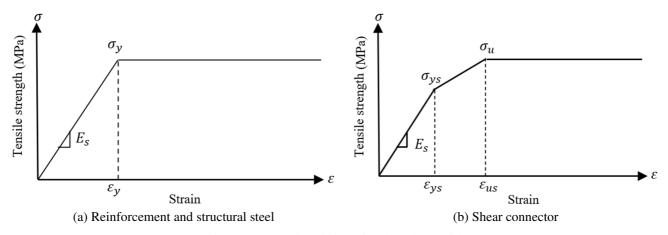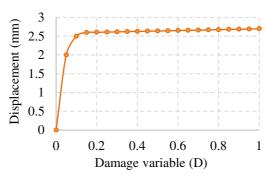
Fig. 9 Stress-strain relationship of steel material

Fig. 10 Damage evolution response

Table 2 PPH stud, structural steel, and rebar material properties

PPH Stud			Structural steel		Rebar	
E_s (GPa)	σ_y (MPa)	σ_u (MPa)	E_s (GPa)	σ_y (MPa)	E_s (GPa)	σ_y (MPa)
216.2	410	466	200	320	210	510

2.6. Verification of FE model

In this study, the pushout experimental setup of Loh et al. [26] is used. The third test is considered for FE modeling. The geometrical and material properties of the 19 mm diameter and 100 mm height circular-headed stud are taken from the literature by Loh et al. [26]. The stud modulus of elasticity was 2.162 GPa at 0.2 percent proof stress of 410 N/mm^2, with 466 N/mm^2 tensile strength and 16.1 percent elongation [26]. The experimental results showed that the third test was used to validate the FE analysis results of the present modeling [26]. The support constraint is eased in this work by lowering the friction coefficient in the contact surface interaction between the concrete slab and base block to 0.15 [21]. For experimental and FE analyses, the maximum load and corresponding slip are 111 kN and 4 mm, respectively. The experimental and numerical results of the pushout tests are in good agreement as shown in Fig. 11.
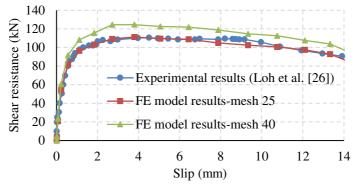

Fig. 11 Comparative verification of the results

3. Parametric Study

The parameters considered for the study are headed stud diameter, concrete grade, pennon plate thickness, and height. The types of stud diameter (*d*) used are 16 mm, 19 mm, and 22 mm. The pennon plates of thicknesses 2 mm, 3 mm, and 4 mm are used. The three different concrete grades used are C30, C40, and C50. The pennon plate height is considered as 1/3rd (0.33 *H*) of the total height (*H*) of the stud for 16 mm *d*, 19 mm *d*, and 2/3rd (0.67 *H*) of the total height (*H*) of the stud for 22 mm *d* as shown in Fig. 12. The combinations of the 54 models are analyzed based on the DOE.

(a) 16 mmⵁ (0.33 *H*) (b) 16 mmⵁ (0.67 *H*) (c) 19 mmⵁ (0.33 *H*)

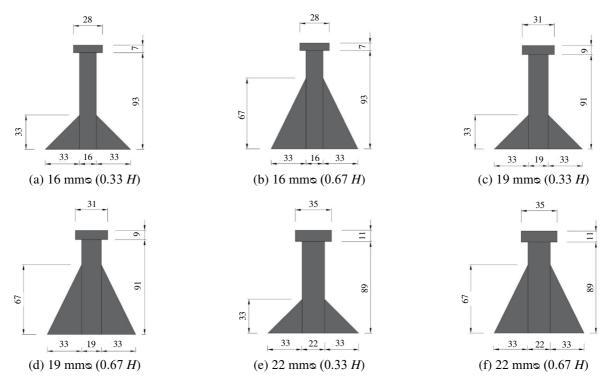(d) 19 mmⵁ (0.67 *H*) (e) 22 mmⵁ (0.33 *H*) (f) 22 mmⵁ (0.67 *H*)

Fig. 12 Parametric details of PPH stud shear connector

DOE is a systematic method for establishing a relationship between the variables influencing a process and its outcome [27]. This study evaluates the performance of shear connectors, such as shear resistance and slip behavior, as an output under the influence of pushout loading for different factors. The factors are headed stud diameter (*d*), grade of concrete (*f_c*), pennon plate thickness (*t*), and the height of the pennon plate (*h*).

The levels are considered low (-), intermediate (I), and high (+). Table 3 shows the variables (factors) and their levels examined in the FE analysis. Furthermore, the effects of *d*, *f_c*, *t*, *h*, and their interactions are investigated using a three-level-three-factor (-, I, + levels and *d*, *f_c*, *t* factors) with two-level-one-factor (-, + levels and *h* factor) full factorial DOE, and analysis of variance (ANOVA).

Thus, a full analysis of $3^3 \times 2^1 = 27 \times 2 = 54$ factor combinations is required. ANOVA is a statistical technique for comparing two or more sets of data [27]. The significance level is set at 0.05. Minitab [28] is used to do statistical analysis on these models and establish run orders.

Table 3 Factors and levels

No.	Factors	Levels		
		Low	Intermediate	High
1	*d* (mm)	16	19	22
2	*f_c* (N/mm²)	30	40	50
3	*t* (mm)	2	3	4
4	*h (mm)*	0.33 *H*	-	0.67 *H*

4. Results and Discussion

The results of FE analysis of pushout tests with various PPH studs and variable concrete strength are compared with the regular-headed stud shear connector. The ultimate load per stud (*P*) and ultimate slip at the failure of 54 pushout specimens are revealed from FE analysis. The total reaction acting on the reference point at the top surface of a steel beam is used to calculate the load. The net difference between the nodes on the steel flange and the nodes on the concrete slab at the stud center is considered for calculating the connection slip. According to the characteristic slip capacity specified by Annex B, Clause B.2.5 of Eurocode 4 [8], the slip for ultimate failure is considered at the point of critical damage when the material or the failure is assumed at the 10% load fell below the ultimate load.

The verification curve as a typical load-slip relationship per stud for pushout specimens of a 19 mm stud diameter is shown in Fig. 11. Table 4 shows the comparison between the load-slip capacity of the PPH studs and the conventional 19 mm circular stud load-slip capacity for C40 and C50 concrete. It can be observed that with the addition of plates to conventional studs, the ultimate strength of the shear connection is increased up to 63% to 77% when utilizing a 2 mm to 4 mm thick plate.

According to Eurocode 4 [8] guidelines, the shear connector is called ductile if the ultimate slip of connection is equal to or more than 6 mm. It can be seen from FEA results that the ductility criteria have been satisfied by all PPH studs and all are justified for practical implementation with advantages increment in ultimate strength. Some descriptive results of FE analysis are elaborated in the following subsection. The significance and interaction of factors based on DOE and ANOVA are also prescribed.

Table 4 Comparisons of the shear resistance of PPH stud with a conventional circular stud

Grade of concrete	Circular stud shear resistance (kN)	PPH studs for 0.33 *H* (kN)		
		2 mm	3 mm	4 mm
C40	136.00	222.03	237.11	242.54
C50	144.83	235.87	256.66	256.63

4.1. Considering the effect of an increase in concrete strength

When a 16 mm diameter stud with 4 mm plate thickness and 1/3rd height of plate is considered as a constant parameter, the shear connection strengths observed are 199.26 kN, 224.86 kN, and 246.15 kN at the concrete grades C30, C40, and C50 respectively. The values of the ultimate slip are observed as 18.08 mm, 16.01 mm, and 15.33 mm respectively.

Hence, with the increase in concrete grade, the ultimate shear resistance of the stud is increased by 12.85% for C40 grade and 23.53% for C50 grade, in comparison with C30 grade concrete as shown in Fig. 13. However, the ultimate connection slip is decreased by 11.44% for C40 and 15.21% for C50 grade.

When a 19 mm diameter stud with 4mm plate thickness and 1/3rd height of the plate is considered as a constant parameter, the shear connection strength for C30 grade concrete is observed as 220.14 kN, and the value of ultimate slip is observed as 20.62 mm. The ultimate shear resistance of the stud is increased by 10.17% for C40 grade and 16.57% for C50 grade, relative to C30 grade concrete. However, the ultimate connection slip is decreased by 2% for C40 and 26% for C50 grade.

When a 22 mm diameter stud with 4 mm plate thickness and 1/3rd height of plate is considered as a constant parameter, the shear connection strength for C30 grade concrete is observed as 227.35 kN, and the value of ultimate slip is observed as 19.37 mm. The ultimate shear resistance of the stud is increased by 9.68% for C40 grade and 15% for C50 grade, relative to C30 grade concrete. In contrast, the ultimate connection slip is decreased by 4.59% for C40 and 34.53% for C50 grade. Based on the above results, it can be stated that the shear resistance of composite connections increases when the strength of the concrete of the RC slab increases, while the ultimate slip at failure decreases.
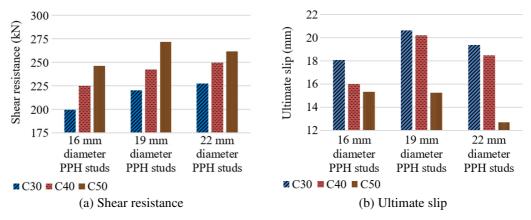
(a) Shear resistance   (b) Ultimate slip

Fig. 13 The effect of the grade of concrete on shear resistance and ultimate slip
performance of the composite connection

4.2. Considering the effect of an increase in headed stud diameter

When a 2 mm plate thickness with C40 concrete grade and 1/3rd height of plate is considered as a constant parameter, with the increase of stud diameters such as 16 mm, 19 mm, and 22 mm, the shear connection strengths observed are 219.77 kN, 222.03 kN, and 237.46 kN, respectively, and the values of ultimate slip are observed as 22.08 mm, 22.51 mm, and 21.62 mm respectively. The ultimate shear resistance of the stud is increased by 1.02% for 19 *d* and 8.04% for 22 *d*, for the 16 *d* stud as shown in Fig. 14. Whereas the ultimate connection slip is increased by 1.94% for 19 *d* and decreased by 2.08% for 22 *d*, in comparison with 16 *d* stud.

When a 3 mm plate thickness with C40 concrete grade and 1/3rd height is considered a constant parameter, the shear connection strength of 16 *d* stud is observed as 219.25 kN, and the value of ultimate slip is observed as 13.92 mm. The ultimate shear resistance of the stud is increased by 8.14 % for 19 *d* stud and 11.31% for 22 *d* stud, for 16 *d* stud. As for, the ultimate connection slip, it is increased by 18.17% for 19 *d* and 46.47% for 22 *d* stud, in comparison with 16 *d* stud.

When a 4 mm plate thickness with C40 concrete grade and 1/3rd height is considered a constant parameter, the shear connection strength of 16 *d* stud is observed as 224.86 kN, and the value of ultimate slip is observed as 16.01 mm. Here, with the increase in shank diameter of the PPH stud, the ultimate shear resistance of the stud is increased by 7.85% for 19 *d* stud and 10.90% for 22 *d* stud, for 16 *d* stud. However, the ultimate connection slip is increased by 25.92% for 19 *d* and 15.49% for 22 *d* stud, in comparison with 16 *d* stud.

From the above observations, it can be concluded that the shear resistance of the connection increases with the increase of stud diameter, whereas no specific pattern is observed for the maximum slip at failure. And an interaction study (ANOVA) has been required to find the influence of main factors and their interaction.
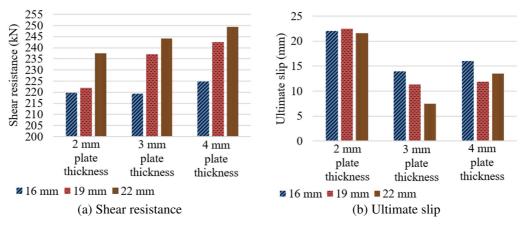

(a) Shear resistance   (b) Ultimate slip

Fig. 14 The effect of stud diameter on shear resistance and ultimate slip
performance of the composite connection

4.3.   Considering the effect of an increase in headed plate thickness

When a 16 mm diameter stud with C50 concrete grade and 2/3rd height of plate is considered as a constant parameter, with the increase of plate thickness such as 2 mm, 3 mm, and 4 mm, the shear connection strengths observed are 232.25 kN, 250.17 kN, and 253.57 kN, respectively. The values of the ultimate slip are observed as 12.16 mm, 9.55 mm, and 19.06 mm respectively as shown in Fig. 15.

Therefore, with the increase in thickness of the pennon plate, the ultimate shear strength of the stud increased by 7.71% for 3 *t,* and 9.17% for 4 *t*, in comparison with 2 *t* plate thickness PPH stud. And, the ultimate connection slip is decreased by 21.46% for 3 *t* and increased by 56.74% for 4 *t*, in comparison with 2 *t* plate thickness PPH stud.

When a 19 mm diameter stud with C50 concrete grade and 2/3rd height of plate is considered a constant parameter, the shear connection strength of 2 *t* plate thickness PPH stud is observed as 250.09 kN, and the value of ultimate slip is observed as 10.48 mm.

Here, with the increase in the pennon plate thickness of the PPH stud, the ultimate shear resistance of the stud is increased by 1.86% for 3 *t* stud and 3.75% for 4 *t* stud, 2 *t* plate thickness PPH stud. However, the ultimate connection slip is increased by 92.17% for 3 *t* and 35.68% for 4 *t* stud, in comparison with 2 *t* plate thickness PPH stud.

When a 22 mm diameter stud with C50 concrete grade and 2/3rd height of plate is considered as a constant parameter, the shear connection strength of 2 *t* plate thickness PPH stud observed is 265.26 kN, and the value of ultimate slip is observed as 18.58 mm. Here, with the increase in the pennon plate thickness of the PPH stud, the ultimate shear resistance of the stud is increased by 1.13% for 3 *t* stud and 1.28% for 4 *t* stud, in comparison with 2 *t* plate thickness PPH stud. Whereas, the ultimate connection slip is decreased by 37.94% for 3*t* and 54.46% for 4*t* stud, in comparison with 2 *t* plate thickness PPH stud.

From the above observations, it can be concluded that the shear resistance of connection is not much affected by the increase of plate thickness in PPH studs. Whereas the maximum slip at failure is influential due to changes in thickness; thus, an interaction study has been required to find the interaction effect of plate thickness with other main factors.
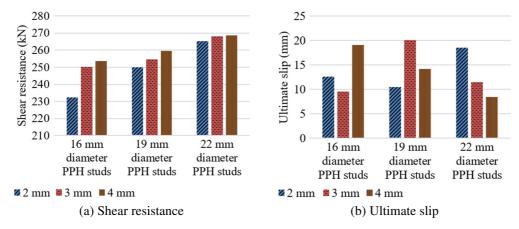

(a) Shear resistance   (b) Ultimate slip

Fig. 15 The effect of the thickness of the PPH plate on shear resistance and
ultimate slip performance of the composite connection

4.4.   Considering the effect of an increase in pennon plate height

When a 16 mm diameter stud with C40 concrete grade and 3 mm plate thickness is considered as a constant parameter, with the increase of the pennon plate height from 1/3rd of total height to 2/3rd of total height, the shear connection strengths observed are 219.25 kN and 224.84 kN respectively, and the values of ultimate slip are observed as 13.92 mm and 10.72 mm respectively. Hence, with the increase in the height of the pennon plate, the ultimate shear resistance of the stud is increased by 1.02% for 0.67 *H*, for 0.33 *H* plate height PPH stud as shown in Fig. 16. And, the ultimate connection slip is decreased by 29.85% for 0.67 *H*.

When a 19 mm diameter stud with C40 concrete grade and 3 mm plate thickness is considered as a constant parameter, with the increase of the pennon plate height from 1/3rd of total height to 2/3rd of total height, the shear connection strengths are observed as 237.11 kN and 236.85 kN respectively, and the values of ultimate slip are observed as 16.44 mm, and 20.37 mm respectively. Thus, with the increase in height of the pennon plate, the ultimate shear resistance of the stud is almost the same for 0.67 *H*. Whereas the ultimate connection slip is decreased by 23.90% for 0.67 *H*.

When a 22 mm diameter stud with C40 concrete grade and 3 mm plate thickness is considered as a constant parameter, with the increase of pennon plate height from 1/3rd of total height to 2/3rd of total height, the shear connection strengths observed are 244.05 kN and 256.22 kN respectively, and the values of ultimate slip are observed as 20.38 mm, and 17.98 mm respectively. Therefore, with the increase in the height of the pennon plate, the ultimate shear resistance of the stud is increased by 4.98% for 0.67 *H*. However, the ultimate connection slip is decreased by 11.77% for 0.67 *H*.

From the above observations, it can be concluded that the increase of pennon plate height from 0.33 *H* to 0.67 *H* for the shear resistance of the connection is not much effective compared to other factors, and a future study is needed on the effect of the height of pennon plate (below 0.33 *H*) on strength capacity of PPH stud. Whereas the maximum slip at failure is influential due to changes in thickness; thus, an interaction study has been required to find the interaction effect of plate height with other main effective factors.
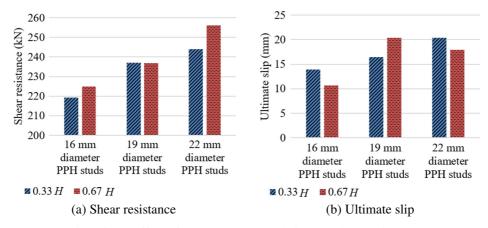

(a) Shear resistance   (b) Ultimate slip

Fig. 16 The effect of PPH pennon plate height on shear resistance
and ultimate slip performance of the composite connection

4.5. The effect of critical factors on shear connectors performance based on DOE and ANOVA

For a total of 54 specimens run, a pushout FE analysis is performed for each combination of three levels of the three factors and two levels of one factor. Fig. 11 depicts a typical pushout analysis result for a high level of each factor, the two performance output responses, ultimate strength of connection, and failure slip. ANOVA can investigate the main effects of input factors and potential interactions on the response variable [27]. This approach separates the dominant factors and interactions that affect the response variable from the less critical factors and interactions, identifying which factors significantly affect the response [27]. As a result, ANOVA analysis is performed to examine the primary influence of four variables and potential interactions at a significance level (*α*) of 5% using a two-sided confidence interval.

The conclusions are drawn from the *P*-value. The *P*-value is the lowest threshold α at which the data are statistically significant [27]. Each effect with a *P*-value less than 0.05 is deemed to have a statistically significant impact on the response with 95% confidence. Table 5 shows the results of an ANOVA study for shear carrying capacity and ultimate slip at various limiting variables. As presented in Table 5, the main effects of f_c and *d* have *P*-values of less than the 5% significance level. Therefore, these factors significantly affect the shear capacity of the connection. Moreover, the main effect of f_c, *h*, and interaction between *t* and *h* considerably affect the ultimate slip capacity of the PPH stud connection.

Table 5 Influence of key parameters on shear resistance and ultimate slip of connector based on ANOVA

Descriptions	No.	Parameters and interactions	P-values	
			Shear resistance	Ultimate slip
Main parameters effect	1	Concrete grade (f_c)	< 0.0001	0.004
	2	Headed stud diameter (d)	< 0.0001	0.818
	3	The thickness of the pennon plate (t)	0.212	0.524
	4	Height of pennon plate (h)	0.395	0.015
Two-way interactions	5	$f_c \times d$	0.305	0.119
	6	$f_c \times t$	0.980	0.996
	7	$f_c \times h$	0.997	0.907
	8	$d \times t$	0.976	0.087
	9	$d \times h$	0.718	0.917
	10	$t \times h$	0.982	0.004

Fig. 17 describes the effect of the main interaction of factors on the ultimate slip of connection. It can be concluded that the main effect of concrete strength, the height of the plate, and the interaction between the thickness and height of the pennon plate significantly affect the ultimate slip capacity of the PPH stud connection.
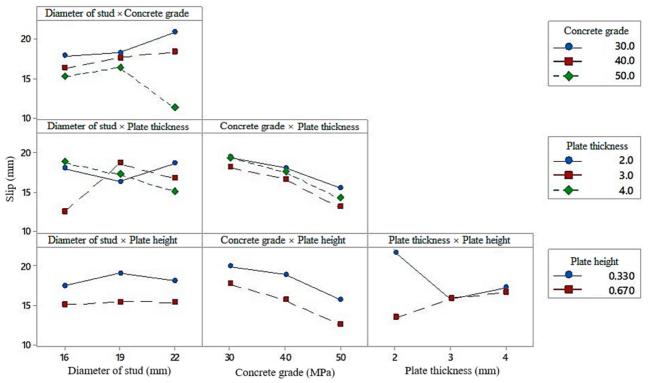

Fig. 17 Interaction plot for ultimate slip

5. Conclusions

A nonlinear FE model was developed to investigate the capacity of an innovative pennon plate-headed (PPH) stud shear connector. The connection capacity and the load-slip behavior were calculated as a performance evaluation. The proposed FE analysis model conducted a parametric study for 54 pushout specimens with different concrete grades, stud diameters, plate thicknesses, and plate heights. The full factorial statistical method and ANOVA were used to design experiments and to evaluate the interaction performance of factors and responses. From the parametric study, the following results are extracted:

(1) The FE model successfully anticipates the behavior of the headed stud shear connection in composite beams with solid slabs and accurately verified the experimental results of prior research. The ultimate strength of the shear connection was improved, and the corresponding slip was affected by adding the pennon plates to the circular-headed stud.

(2) When PPH studs are utilized with C40 and C50 concrete grades, the connection ultimate shear strength increases by 63% to 77% due to the change in stud shape from regular circular-headed studs to PPH studs.

(3) All PPH studs meet the ductility requirements specified in Eurocode 4 [8]. Therefore, they are justified for practical application with advantages increment in the ultimate strength.

(4) The full factorial analysis reveals that the effects of the concrete grade of the RC slab and stud diameter on the ultimate strength were highly significant. The shear resistance of the connection increases with the stud diameter increases.

(5) The effect of interaction among factors on the shear resistance response of PPH stud has no significant influence. However, the interaction of $t \times h$ was shown to have a highly significant influence on the slip performance of the PPH shear connection. The shear resistance of the connection is not much affected by the increase of plate thickness above 3 mm in PPH studs. Whereas the maximum slip at failure is influential due to changes in thickness.

(6) The PPH stud shear connectors are suitable for composite structures due to their ability to enhance the shear resistance capacity of the connection.

Abbreviations and Symbols

3D	Three-dimensional	E_{cm}	Modulus of elasticity
ANOVA	Analysis of variance	ε_{ctr}	Cracking strain
CDP	Concrete damage plasticity	f_c	Grades of concrete
DOE	Design of experiments	f_{cm}	Cylindrical compressive strength
FE	Finite element	f_{ct}	Concrete tensile strength
PPH	Pennon plate-headed	f_{cu}	Cube compressive strength of concrete
RC	Reinforced concrete	h	Height of pennon plate
D	Damage variable	k	deviatoric cross-section parameter
D_c	Compression damage	t	Pennon plate thickness
D_t	Tension damage	σ_u	Ultimate stress
d	Stud diameter	σ_y	Yield stress
SBC	Symmetric boundary condition	P	Ultimate load per stud
H	Total height of PPH stud		

Conflicts of Interest

The authors declare no conflict of interest.

References

[1] R. T. Pardeshi and Y. D. Patil, "Review of Various Shear Connectors in Composite Structures," Advanced Steel Construction, vol. 17, no. 4, pp. 394-402, December 2021.

[2] J. G. Ollgaard, R. G. Slutter, and John W. Fisher, "Shear Strength of Stud Connectors in Lightweight and Normal Weight Concrete," Engineering Journal, American Institute of Steel Construction, vol. 8, pp. 55-64, April 1971.

[3] I. M. Viest, "Investigation of Stud Shear Connectors for Composite Concrete and Steel T-Beams," ACI Journal Proceedings, vol. 52, no. 4, pp. 875-892, April 1956.

[4] Q. Sun, X. Nie, M. D. Denavit, J. S. Fan, and W. Liu, "Monotonic and Cyclic Behavior of Headed Steel Stud Anchors Welded through Profiled Steel Deck," Journal of Constructional Steel Research, vol. 157, pp. 121-131, June 2019.

[5] W. Q. Deng, J. C. Gu, D. Liu, J. Hu, and J. D. Zhang, "Study of Single Perfobond Rib with Head Stud Shear Connectors for a Composite Structure," Magazine of Concrete Research, vol. 71, no. 17, pp. 920-934, September 2019.

[6] M. Konrad and U. Kuhlmann, "Headed Studs Used in Trapezoidal Steel Sheeting According to Eurocode 4," Structural Engineering International: Journal of the International Association for Bridge and Structural Engineering, vol. 19, no. 4, pp. 420-426, 2009.

[7] L. Z. Chen, G. Ranzi, S. C. Jiang, F. Tahmasebinia, and G. O. Li, "Performance and Design of Shear Connectors in Composite Beams with Parallel Profiled Sheeting at Elevated Temperatures," International Journal of Steel Structures, vol. 16, no. 1, pp. 217-229, March 2016.

[8] Eurocode 4: Design of Composite Steel and Concrete Structures – Part 1-1: General Rules and Rules for Buildings, EN 1994-1-1, 2004.

[9] Y. Imagawa, O. Ohyama, and A. Kurita, "Mechanical Properties of Shear Stud during and after Fire," Structural Engineering International, vol. 22, no. 4, pp. 487-492, 2012.

[10] C. S. Shim and D. W. Kim, "Structural Performance of Composite Joints Using Bent Studs," International Journal of Steel Structures, vol. 10, no. 1, pp. 1-13, March 2010.

[11] A. S. H. Suwaed and T. L. Karavasilis, "Novel Demountable Shear Connector for Accelerated Disassembly, Repair, or Replacement of Precast Steel-Concrete Composite Bridges," Journal of Bridge Engineering, vol. 22, no. 9, article no. 0001080, September 2017.

[12] A. S. H. Suwaed and T. L. Karavasilis, "Demountable Steel-Concrete Composite Beam with Full-Interaction and Low Degree of Shear Connection," Journal of Constructional Steel Research, vol. 171, article no. 106152, August 2020.

[13] S. W. Pathirana, B. Uy, O. Mirza, and X. Q. Zhu, "Bolted and Welded Connectors for the Rehabilitation of Composite Beams," Journal of Constructional Steel Research, vol. 125, pp. 61-73, October 2016.

[14] F. Yang, Y. Q. Liu, Zh. B. Jiang, and H. H. Xin, "Shear Performance of a Novel Demountable Steel-Concrete Bolted Connector under Static Push-Out Tests," Engineering Structures, vol. 160, pp. 133-146, April 2018.

[15] O. Mirza and B. Uy, "Effects of Strain Regimes on the Behaviour of Headed Stud Shear Connectors for Composite Steel-Concrete Beams," Advanced Steel Construction, vol. 6, no. 1, pp. 635-661, 2010.

[16] J. Qureshi, D. Lam, and J. Q. Ye, "The Influence of Profiled Sheeting Thickness and Shear Connector's Position on Strength and Ductility of Headed Shear Connector," Engineering Structures, vol. 33, no. 5, pp. 1643-1656, May 2011.

[17] V. Vigneri, C. Odenbreit, and M. Braun, "Numerical Evaluation of the Plastic Hinges Developed in Headed Stud Shear Connectors in Composite Beams with Profiled Steel Sheeting," Structures, vol. 21, pp. 103-110, October 2019.

[18] M. M. Mia and A. K. Bhowmick, "A Finite Element Based Approach for Fatigue Life Prediction of Headed Shear Studs," Structures, vol. 19, pp. 161-172, June 2019.

[19] R. T. Pardeshi, P. A. Singh, and Y. D. Patil, "Performance Assessment of Innovative Concave Type Shear Connector in a Composite Structure Subjected to Push-Out Loading," Materials Today: Proceedings, vol. 65, no. 2, pp. 676-680, 2022.

[20] "Abaqus 6.11, Abaqus/CAE User's Manual," http://130.149.89.49:2080/v6.11/pdf_books/CAE.pdf, March 01, 2021.

[21] H. T. Nguyen and S. E. Kim, "Finite Element Modeling of Push-Out Tests for Large Stud Shear Connectors," Journal of Constructional Steel Research, vol. 65, no. 10-11, pp. 1909-1920, October-November 2009.

[22] Eurocode 2: Design of Concrete Structures – Part 1-1: European Committee for Standardization, EN 1994-1-1, 2004.

[23] E. Ellobody, B. Young, and D. Lam, "Behaviour of Normal and High Strength Concrete-Filled Compact Steel Tube Circular Stub Columns," Journal of Constructional Steel Research, vol. 62, no. 7, pp. 706-715, July 2006.

[24] T. Wang and T. T. Hsu, "Nonlinear Finite Element Analysis of Concrete Structures Using New Constitutive Models," Computers & Structures, vol. 79, no. 32, pp. 2781-2791, December 2001.

[25] B. Alfarah, F. López-Almansa, and S. Oller, "New Methodology for Calculating Damage Variables Evolution in Plastic Damage Model for RC Structures," Engineering Structures, vol. 132, pp. 70-86, February 2017.

[26] H. Y. Loh, B. Uy, and M. A. Bradford, "The Behaviour of Composite Beams in Hogging Moment Regions – Part I: Experimental Study," The University of New South Wales, UNICIV Report No. R-418, April 2003.

[27] D. C. Montgomery, Design and Analysis of Experiments, 9th ed., New Jersey: John Willy & Sons, 2017.

[28] "Minitab 18 Statistical Software," https://www.minitab.com/en-us/, March 01, 2021.